Ground-state degeneracy of Potts antiferromagnets: cases with noncompact *W* boundaries having multiple points at $1/q = 0$

1998 J. Phys. A: Math. Gen. 31 9641

(http://iopscience.iop.org/0305-4470/31/48/003)

J. Phys. A: Math. Gen. **31** (1998) 9641–9665. Printed in the UK PII: S0305-4470(98)96911-6

Ground-state degeneracy of Potts antiferromagnets: cases with noncompact W boundaries having multiple points at $1/q = 0$

Robert Shrock† and Shan-Ho Tsai‡

Institute for Theoretical Physics, State University of New York, Stony Brook, NY 11794-3840, USA

Received 20 August 1998

Abstract. We present exact calculations of the zero-temperature partition function, $Z(G, q, T = 0)$, and ground-state degeneracy (per site), $W(\{G\}, q)$, for the q-state Potts antiferromagnet on a number of families of graphs $\{G\}$ for which the boundary $\mathcal{B}$ of regions of analyticity of W in the complex q-plane is noncompact and has the properties that (i) in the $z = 1/q$-plane, the point $z = 0$ is a multiple point on $\mathcal{B}$ and (ii) $\mathcal{B}$ includes support for $\mathrm{Re}\,(q) < 0$. These families are generated by the method of homeomorphic expansion. Our results give further insight into the conditions for the validity of large-q series expansions for the reduced function $W_{\mathrm{red}} = q^{-1}W$.

1. Introduction

This paper continues our study of nonzero ground-state entropy, $S_0(\{G\}, q) \neq 0$, i.e. ground-state degeneracy (per site) $W(\{G\}, q) > 1$, where $S_0 = k_B \ln W$, in q-state Potts antiferromagnets [1, 2] on various lattices and, more generally, families of graphs $\{G\}$. There is an interesting connection with graph theory here, since the zero-temperature partition function of the above-mentioned q-state Potts antiferromagnet on a graph G satisfies $Z(G, q, T = 0)_{PAF} = P(G, q)$, where $P(G, q)$ is the chromatic polynomial expressing the number of ways of colouring the vertices of the graph G with q colours such that no two adjacent vertices have the same colour [3–6]. Thus,

$$W\Big(\Big[\lim_{n\to\infty} G\Big], q\Big) = \lim_{n\to\infty} P(G, q)^{1/n} \tag{1.1}$$

where $n = v(G)$ is the number of vertices of G. An example of a real substance exhibiting nonzero ground-state entropy is ice [7, 8]. Just as complex analysis provides deeper insights into real analysis in mathematics, the generalization from $q \in \mathbb{Z}_+$, to $q \in \mathbb{C}$ yields a deeper understanding of the behaviour of $W(\{G\}, q)$ for physical (positive integral) q. In general, $W(\{G\}, q)$ is an analytic function in the q-plane except along a certain continuous locus of points, which we denote $\mathcal{B}$ (and at possible isolated singularities which will not be relevant here). In the limit as $n \to \infty$, the locus $\mathcal{B}$ forms by means of a coalescence of a subset of the zeros of $P(G, q)$ (called chromatic zeros of G) [9]. In a series of papers we have

† E-mail address: shrock@insti.physics.sunysb.edu

‡ Current address: Department of Physics and Astronomy, University of Georgia, Athens, GA 30602, USA. E-mail address: tsai@hal.physast.uga.edu

calculated and analysed $W(\{G\}, q)$ for a variety of families of graphs [11–16], both for physical values of q (via rigorous upper and lower bounds, large-q series calculations, and Monte Carlo measurements) and for the generalization to complex values of q.

A basic question that one can ask about the locus $\mathcal{B}$ for the ($n \to \infty$ limit of a) family of graphs $\{G\}$ is whether it extends only a finite distance from the origin of the q-plane or, instead, extends an infinite distance away from this origin (i.e. passes through the point $z = 0$ in the $z = 1/q$-plane), and hence is noncompact. The importance of this question for the statistical mechanics of q-state Potts antiferromagnets is that large-q Taylor series provide a powerful means of obtaining approximate values of the ground-state degeneracy even for moderate values of q [17–19, 14, 15], but these exist if and only if the reduced function $W_{\mathrm{red}}(\{G\}, q) = q^{-1}W(\{G\}, q)$† is analytic at $1/q = 0$, which, in turn, is true if and only if the nonanalytic boundary $\mathcal{B}$ does not pass through $z = 0$. Large-q series calculations of W_{red} have been derived for regular lattices [17–19], but we noted [12] that for the $r \to \infty$ limit of the graph $\overline{K}_2 + C_r$ the locus $\mathcal{B}$, which is noncompact [10], no such large-q series exists. Here, $\overline{K}_p$ denotes the complement of the complete graph K_p‡. It is clearly important to understand better the differences between the behaviour of Potts antiferromagnets on families of graphs that yield $W_{\mathrm{red}}(\{G\}, q)$ functions analytic at $z = 0$ and those that do not, i.e. those that yield noncompact loci $\mathcal{B}$ passing through $z = 0$ [13]. In this paper, we carry out such a study for families of graphs which are homeomorphic expansions of the following type. We start with families of the form $(K_p)_b + G_r$, where G_r is a given graph family with r vertices, b signifies the removal of certain bonds in the K_p subgraph, and $G + H$ is the 'join' of the graphs G and H§. We then perform *homeomorphic expansion* of the bonds *connecting* the K_p and G_r subgraphs. This family is categorized as being of type HEC. An interesting feature of the families analysed here is that, in contrast to those that we have previously studied, they yield loci $\mathcal{B}$ (which are boundaries of regions of analyticity of W) that have support for $\mathrm{Re}(q) < 0$ and for which the point $z = 0$ is a multiple point on the algebraic curve $\mathcal{B}$ in the technical terminology of algebraic geometry [20], i.e. a point where several branches of this curve cross each other. For basic definitions on homeomorphic classes of graphs, see [6]; some recent work on homeomorphism classes in a different direction than ours is [22].

A general form for the chromatic polynomial of an n-vertex graph G is

$$P(G, q) = c_0(q) + \sum_{j=1}^{N_a} c_j(q) a_j(q)^{t_j n} \tag{1.2}$$

where $c_j(q)$ and $a_j(q)$ are certain functions of q. Here the $a_j(q)$ and $c_{j\neq 0}(q)$ are independent of n, while $c_0(q)$ may contain n-dependent terms, such as $(-1)^n$, but does not grow with n like (constant)^n. A term $a_\ell(q)$ is defined as 'leading' if it dominates the $n \to \infty$ limit of $P(G, q)$; in particular, if $N_a \geqslant 2$, then it satisfies $|a_\ell(q)| \geqslant 1$ and $|a_\ell(q)| > |a_j(q)|$ for $j \neq \ell$, so that $|W| = |a_\ell|^{t_j}$. The locus $\mathcal{B}$ occurs where there is a nonanalytic change in W as the leading terms a_ℓ in equation (1.2) changes.

† This reduced function is a natural object to define since an obvious upper bound on $P(G, q)$ describing the colouring of an n-vertex graph with q colours is $P(G, q) \leqslant q^n$, and hence $W(\{G\}, q) \leqslant q$; this guarantees that $\lim_{q\to\infty} W_{\mathrm{red}}(\{G\}, q)$ is a finite quantity (even if it is sometimes nonanalytic at this point). The large-q series take their simplest form as series in the expansion variable $y = 1/(q - 1)$ for the equivalent reduced function $\overline{W}(\{G\}, q) = q^{-1}(1 - q^{-1})^{-\Delta/2} W(\{G\}, q)$, where Δ is the coordination number of the lattice.

‡ The complete graph K_n on n vertices is defined as the graph where each of these vertices is connected to all of the other $n - 1$ vertices by bonds. The complement $\overline{K}_n$ of K_n is the graph with n vertices and no bonds.

§ The 'join' of two graphs G and H is obtained by adding bonds connecting each of the vertices of G to those of H. This was denoted $G \times H$ in [13]; here we use the more common notation for this object in the mathematical literature, namely $G + H$.

Since for the families of graphs studied here, the boundary $\mathcal{B}$ is noncompact in the q-plane, it is often more convenient to describe the boundary in the complex z- or y-planes, where, as above, $z = 1/q$, and

$$y \equiv \frac{1}{q-1} = \frac{z}{1-z}. \tag{1.3}$$

The variable y is commonly used in large-q series expansions. For the families considered here $\mathcal{B}$ is actually compact in the y- and z-planes. We define polar coordinates as

$$z = \zeta \mathrm{e}^{\mathrm{i}\theta} \tag{1.4}$$

and

$$y = \rho \mathrm{e}^{\mathrm{i}\beta} \tag{1.5}$$

and the function

$$D_k(q) = \frac{P(C_k, q)}{q(q-1)} = a^{k-2} \sum_{j=0}^{k-2} (-a)^{-j} = \sum_{s=0}^{k-2} (-1)^s \binom{k-1}{s} q^{k-2-s} \tag{1.6}$$

where $a = q - 1 = 1/y$ and $P(C_k, q)$ is the chromatic polynomial for the circuit (cyclic) graph C_k with k vertices,

$$P(C_k, q) = a^k + (-1)^k a. \tag{1.7}$$

We shall also use a standard notation from combinatorics,

$$q^{(p)} = p! \binom{q}{q-p} = \prod_{s=0}^{p-1} (q - s). \tag{1.8}$$

The organization of this paper is as follows. In section 2 we construct several general multiparameter homeomorphic classes of families of graphs that, in a certain limit, yield noncompact boundaries $\mathcal{B}(q)$. In sections 3–5 we give exact calculations of the respective boundaries $\mathcal{B}$ for three such families. These exhibit features going beyond those that we found in our earlier work in three main ways: (i) the point $z = 0$ can be a multiple point; (ii) $\mathcal{B}$ includes support for $\mathrm{Re}\,(q) < 0$, and (iii) it is no longer true in general that $\mathrm{Re}\,(q) = 0 \Leftrightarrow q = 0$ for $q \in \mathcal{B}$. A general discussion of our findings is given in section 6, and our conclusions are presented in the final section.

2. Homeomorphic classes of HEC type

We can construct a large variety of families of graphs with noncompact boundaries $\mathcal{B}(q)$ of regions where the respective W-functions are analytic by performing homeomorphic expansions of the basic family constructed and analysed before [13]:

$$(K_p)_b + G_r \tag{2.1}$$

where, as before, b denotes the removal of b bonds connecting a vertex v in the K_p subgraph to the other vertices of K_p. Since each vertex $v \in K_p$ has degree $\Delta = p - 1$, b is bounded above according to $b \leqslant p - 1$. We have shown earlier that (i) the locus $\mathcal{B}$ for $\lim_{r\to\infty}[(K_p)_b + G_r]$ is noncompact in the q-plane, passing through $z = 1/q = 0$ [13] and (ii) the analogous locus for the $r \to \infty$ limit of homeomorphic expansions of this family has the same noncompactness property. To construct specific homeomorphic expansions, select a vertex v_1 in the K_p subgraph and perform homeomorphic expansion on each of the bonds connecting this vertex with the vertices in G_r by inserting $k_1 - 2$ additional degree-two vertices on each of these bonds, where $k_1 \geqslant 3$. Then continue this process with a second

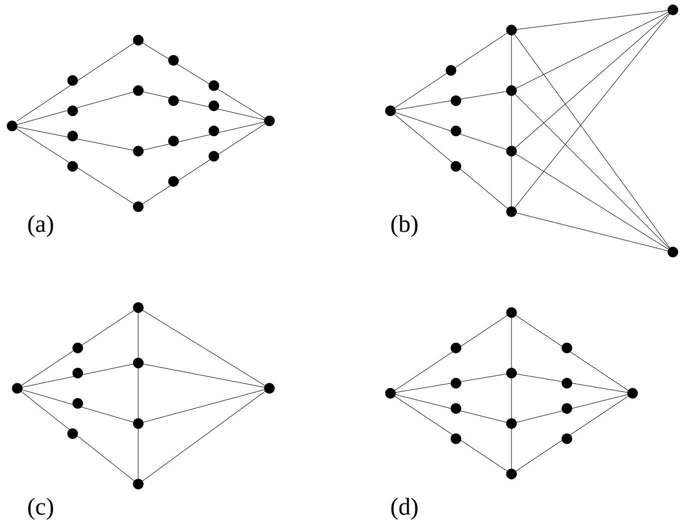

Figure 1. Illustrations of families of graphs considered in the text: (a) $H_{k,r} = HEC_{k_1-2,k_2-2}(\overline{K}_2+\overline{K}_r)$, with $r=4$ and $k_1=3$, $k_2=4$, whence $k=k_1+k_2-1=6$; (b) $\Theta_{k_1,r} = HEC_{k_1-2,0,0}(\overline{K}_3+T_r)$ with $k_1=3$ and $r=4$; (c) $O_{k_1,r} = HEC_{k_1-2,0}(\overline{K}_2+T_r)$ with $k_1=3$ and $r=4$; (d) $U_{k,r} = HEC_{k_1-2,k_2-2}(\overline{K}_2+T_r)$ with $k_1=k_2=k=3$ and $r=4$. Here, K_p is the complete graph with p vertices and T_r is the tree graph with r vertices.

vertex $v_2 \in K_p$, inserting k_2-2 additional degree-two vertices on each of bonds connecting v_2 with the vertices of G_r, and so forth for the other vertices in K_p (including the vertex v from which the b bonds were removed. We denote the resultant homeomorphic expansion as

$$HEC_{k_1-2,k_2-2,\ldots,k_p-2}[(K_p)_{b(v)}+G_r]. \tag{2.2}$$

The labelling is chosen so that, counting the two vertices on the original bond connecting to $v_j \in K_p$ together with the k_j-2 inserted vertices, there is a total of k_j vertices in what was originally this single bond. Some illustrative examples of this and other types of families to be discussed are shown in figure 1.

Another starting family with a noncompact $\mathcal{B}$ in the $r \to \infty$ limit is

$$(K_p)_{\{b\};\{v\}}+G_r \tag{2.3}$$

where the subscript $\{b\}$ refers to the removal of multiple bonds from a set of non-adjacent vertices $\{v\}$ of the K_p subgraph. Performing the HEC-type homeomorphic expansion as above leads to the family

$$HEC_{k_1-2,k_2-2,\ldots,k_p-2}[(K_p)_{\{b\};\{v\}}+G_r]. \tag{2.4}$$

A special case of equation (2.4) applies if in the starting family one removes all of the bonds connecting vertices in the K_p subgraph to each other, so that this starting family is

$$\overline{K}_p+G_r. \tag{2.5}$$

The HEC-type homeomorphic expansion of this family is thus

$$HEC_{k_1-2,k_2-2,\ldots,k_p-2}(\overline{K}_p+G_r). \tag{2.6}$$

In this case one clearly obtains the same homeomorphically expanded family if one permutes the choices of k_j:

$$HEC_{k_1-2,k_2-2,\ldots,k_p-2}(\overline{K}_p+G_r) = HEC_{\pi(k_1)-2,\pi(k_2)-2,\ldots,\pi(k_p)-2}(\overline{K}_p+G_r) \tag{2.7}$$

where π is an element of the permutation group on p objects, S_p. The number of vertices in the homeomorphic classes of families (2.2), (2.4), and (2.6) is the same, namely

$$v(HEC_{k_1-2,k_2-2,\ldots,k_p-2}[(K_p)_b + G_r]) = v(HEC_{k_1-2,k_2-2,\ldots,k_p-2}[(K_p)_{\{b\};\{v\}} + G_r])$$
$$= v(HEC_{k_1-2,k_2-2,\ldots,k_p-2}[\overline{K}_p + G_r]) = p + r\left(1 - 2p + \sum_{j=1}^{p} k_j\right). \tag{2.8}$$

Note that for $p = 2$, since one can only remove $b = 1$ bond in the K_2 subgraph, thereby obtaining $(K_2)_{b=1} = \overline{K}_2$, it follows also that

$$HEC_{k_1-2,k_2-2}[(K_2)_{b=1} + G_r] = HEC_{k_1-2,k_2-2}[\overline{K}_2 + G_r]. \tag{2.9}$$

For the case $G_r = \overline{K}_r$, the chromatic number is

$$\chi(HEC_{k_1-2,k_2-2,\ldots,k_p-2}[\overline{K}_p + \overline{K}_r]) = 2. \tag{2.10}$$

For $G_r = T_r$, for the cases $r \geqslant 2$ of interest here,

$$\chi(HEC_{k_1-2,k_2-2,\ldots,k_p-2}[\overline{K}_p + T_r]) = 3 \tag{2.11}$$

so that for $r \geqslant 2$,

$$P(HEC_{k_1-2,k_2-2,\ldots,k_p-2}[\overline{K}_p + T_r], q = 2) = 0. \tag{2.12}$$

For the $r = 1$ case, this family degenerates to a tree graph,

$$HEC_{k_1-2,k_2-2,\ldots,k_p-2}[\overline{K}_p + T_1] = T_{v_t} \qquad \text{where } v_t = 1 + \sum_{j=1}^{p}(k_j - 1) \tag{2.13}$$

with chromatic polynomial $P(T_{v_t}, q) = q(q-1)^{v_t - 1}$ and chromatic number $\chi = 2$.

A general result for the chromatic polynomial in the case $r = 2$, $G_r = T_r$ is

$$P(HEC_{k_1-2,k_2-2,\ldots,k_p-2}[\overline{K}_p + T_2], q) = q(q-1)\prod_{j=1}^{p} D_{2k_j-1}. \tag{2.14}$$

Since the respective indices $2k_j - 1$ of each of the D_{2k_j-1} in equation (2.14) are odd and since

$$D_{k\,\mathrm{odd}} = (q-2) \times \mathrm{pol}(q) \tag{2.15}$$

where $\mathrm{pol}(q)$ is a polynomial in q of degree $k-3$, it follows that

$$P(HEC_{k_1-2,k_2-2,\ldots,k_p-2}[\overline{K}_p + T_2], q) = q(q-1)(q-2)^p \times \mathrm{pol}'(q) \tag{2.16}$$

where $\mathrm{pol}'(q)$ is a polynomial of degree $2\sum_{j=1}^{p}(k_j - 2)$.

Since the number of vertices $n = v$ is a linear function of p, r, and $k_1, \ldots, k_p$, there are several ways of producing the limit $n \to \infty$ (L denotes limit):

$$L_p : p \to \infty \qquad \text{with } r, k_1, \ldots, k_p \text{ fixed} \tag{2.17}$$
$$L_r : r \to \infty \qquad \text{with } p, k_1, \ldots, k_p \text{ fixed} \tag{2.18}$$
$$L_{k_j} : k_j \to \infty \qquad \text{with } p, r, k_1, \ldots, k_{j-1}, k_{j+1}, \ldots, k_p \text{ fixed} \tag{2.19}$$

and, for the case where all of the k_j's are the same, i.e. $k_j = k_{\mathrm{cb}} \forall j$ (where the subscript cb denotes 'connecting bond'),

$$L_k : k_{\mathrm{cb}} \to \infty \qquad \text{with } p, r \text{ fixed.} \tag{2.20}$$

As discussed before [13], the limit L_p is not of much interest from the viewpoint of either statistical mechanics or graph theory, since for any given graph G_r and for any given (finite) value of $q \in \mathbb{Z}_+$, as p becomes sufficiently large, one will not be able to colour the graph $(K_p)_b + G_r$ or homeomorphic expansions thereof, and the chromatic polynomial will vanish. The limits L_{k_j} and L_k are also not of primary interest here since they generically yield compact boundaries $\mathcal{B}$, as will be illustrated below. We shall therefore concentrate on the limit L_r. The lowest choice of p that yields a noncompact boundary $\mathcal{B}(q)$ is $p = 2$.

For general p and G_r, we remark on two special types of HEC homeomorphic expansions. A minimal case is one in which the above homeomorphic expansion is carried out only on the bonds connecting a single vertex, taken to be v_1 with no loss of generality, in $\overline{K}_p$ to vertices in G_r, so $k_2 = k_3 = \cdots = k_p = 2$:

$$HEC_{k_1-2,0,\ldots,0}(\overline{K}_p + G_r). \tag{2.21}$$

A particularly symmetric case is the one in which the homeomorphic expansions are the same on all of the connecting bonds:

$$HEC_{k_1-2,k_2-2,\ldots,k_p-2}(\overline{K}_p + G_r) \qquad \text{with } k_1 = k_2 = \cdots = k_p \equiv k_{\mathrm{cb}}. \tag{2.22}$$

In this case, the right-hand side of equation (2.8) reduces to $v = p + r + pr(k_{\mathrm{cb}} - 2)$. We proceed to give detailed analyses of some special families of homeomorphic expansions.

3. Class of families $HEC_{k_1-2,k_2-2}(\overline{K}_2 + \overline{K}_r)$

The family $HEC_{k_1-2,k_2-2}(\overline{K}_2 + \overline{K}_r)$ has the special property that the graphs of this family only depend on the sum of k_1 and k_2, not on each of these parameters individually:

$$HEC_{k_1-2,k_2-2}(\overline{K}_2 + \overline{K}_r) = HEC_{k_1'-2,k_2'-2}(\overline{K}_2 + \overline{K}_r) \Leftrightarrow k_1 + k_2 = k_1' + k_2'. \tag{3.1}$$

To incorporate this symmetry, we define

$$H_{k,r} = HEC_{k-3}(\overline{K}_2 + \overline{K}_r) = HEC_{k_1-2,k_2-2}(\overline{K}_2 + \overline{K}_r) \qquad \text{where } k = k_1 + k_2 - 1. \tag{3.2}$$

As will be evident in our explicit results below, the fact that this family has a noncompact W boundary $\mathcal{B}(q)$ in the L_r limit can be understood to follow from its construction as a homeomorphic expansion of the starting family $(K_2)_{b=1} + G_r = \overline{K}_2 + G_r$ which (as was shown previously [13]) has a noncompact $\mathcal{B}$ (here, $G_r = \overline{K}_r$). The noncompactness of the boundary $\mathcal{B}$ obviously implies that in the L_r limit, the chromatic zeros have unbounded magnitudes (in the q-plane), since $\mathcal{B}$ arises via the coalescence of these chromatic zeros in this limit [13]†. We note that the case $k_1 = k_2 = 2$, i.e. $k = 3$ is a special case of the graphs with noncompact $\mathcal{B}(q)$ that we have constructed and studied before [13], so we concentrate on the homeomorphic expansions $k \geqslant 3$ here. The number of vertices is given by the $p = 2$ special case of equation (2.8) with (3.2), namely $v(H_{k,r}) = (k-2)r + 2$. For arbitrary $k \geqslant 2$ and $r \geqslant 1$, $H_{k,r}$ is bipartite, i.e.

$$\chi(H_{k,r}) = 2. \tag{3.3}$$

For $r \geqslant 2$, the girth is $g(H_{k,r}) = 2k - 2$. Indeed, all (non self-intersecting) closed paths are of this length. For $r = 1$ and $r = 2$, the family degenerates according to

$$H_{k,1} = T_k \tag{3.4}$$

† For a family of graphs $G_{k,r}$, rather than analysing the continuous locus $\mathcal{B}$ resulting from the L_r limit in equation (2.18) or the L_k in equation (2.20), one may formulate a different problem: let $\{q_0\}_{k,r}$ denote the set of chromatic zeros of $G_{k,r}$, and consider the union of this set, summed over both r and k, denoted $\{q_0\}_{\forall k,r} = \sum_{r=1}^{\infty}\sum_{k=2}^{\infty}\{q_0\}_{k,r}$. This problem has been considered for the family $G_{k,r} = H_{k,r}$ by A Sokal, who finds (private communication) that the image of this union is dense in the vicinity of the origin, $y = z = 0$. We thank Professor Sokal for this communication

and

$$H_{k,2} = C_{2k-2} \tag{3.5}$$

where, as defined above, T_n and C_n are, respectively, the tree and circuit graphs with n vertices. Hence, we shall take $r \geqslant 3$.

By use of the deletion-contraction theorem† we obtain the recursion relation

$$P(H_{k,r}, q) = D_k P(H_{k,r-1}, q) + (-1)^{k-1} q[(q-1)D_{k-1}]^{r-1} \tag{3.6}$$

which we solve to get the chromatic polynomial

$$P(H_{k,r}, q) = q(q-1)[D_{2k-2}(D_k)^{r-2} - (q-1)(D_{k-1})^2[(D_k)^{r-2} - \{(q-1)D_{k-1}\}^{r-2}]]. \tag{3.7}$$

This has the form of equation (1.2) with $N_a = 2$,

$$a_1 = D_k \tag{3.8}$$

and

$$a_2 = (q-1)D_{k-1}. \tag{3.9}$$

In the limit L_r of equation (2.18), the nonanalytic boundary locus $\mathcal{B}$ is determined as the solution of the degeneracy of magnitudes of the leading terms

$$|a_1| = |a_2|. \tag{3.10}$$

To determine $\mathcal{B}$, we multiply equation (3.10) by $|q(q-1)|$ to obtain $|P(C_k, q)| = |(q-1)P(C_{k-1}, q)|$ (the resultant spurious solutions thereby introduced at $q = 0, 1$, i.e. $y = -1, \infty$, are understood to be ignored in the following discussion). Dividing by $|a|^k$ yields

$$|1 + (-1)^k y^{k-1}| = |1 + (-1)^{k-1} y^{k-2}|. \tag{3.11}$$

Since $y = 0$ is a solution of equation (3.11), $\mathcal{B}$ is noncompact in the q-plane, passing through $z = 1/q = 0$, as noted above (equivalently, equation (3.10) satisfies the condition given in the theorem of section 4 of [13], that guarantees that the solution locus $\mathcal{B}$ is noncompact in the q-plane). (In contrast, for fixed k, $\mathcal{B}$ is compact in the z- or y-plane.)

Furthermore, we find that (i) $2(k-2)$ curves on $\mathcal{B}$, consisting of $(k-2)$ complex-conjugate (c.c.) pairs, intersect at $z = y = 0$; (ii) these curves approach the point $z = y = 0$ at the angles

$$\phi_j = \beta_j = \pm\frac{(2j+1)\pi}{2(k-2)} \qquad j = 0, \ldots, k-3. \tag{3.12}$$

Thus, if and only if k is odd, these angles include $\pm\pi/2$, i.e. a branch of $\mathcal{B}$ crosses the point $z = y = 0$ vertically. To prove these results, we write (3.11) in terms of polar coordinates using equation (1.5):

$$\rho^{k-2}[\rho^{k-2}(\rho^2 - 1) + 2(-1)^k\{\rho\cos[(k-1)\beta] + \cos[(k-2)\beta]\}] = 0. \tag{3.13}$$

As $\rho \to 0$, so that $z \to y$ (whence $\beta \to \phi$), the solution is given by $\cos[(k-2)\beta] = 0$, which yields the results (i) and (ii). In the terminology of algebraic geometry [20], the point $z = y = 0$ is a singular (multiple) point on the algebraic curve $\mathcal{B}$ of index $k-2$.

† We recall the statement of the addition-contraction theorem [4–6]: let G be a graph, and let v and v' be two nonadjacent vertices in G. Form (i) the graph G_{add} in which one adds a bond connecting v and v', and (ii) the graph G_{contr} in which one identifies v and v'. Then the chromatic polynomial for colouring G with q colours, $P(G, q)$, satisfies $P(G, q) = P(G_{\mathrm{add}}, q) + P(G_{\mathrm{contr}}, q)$. The reverse process of bond deletion, leading to the same equation, is known as the deletion-contraction theorem.

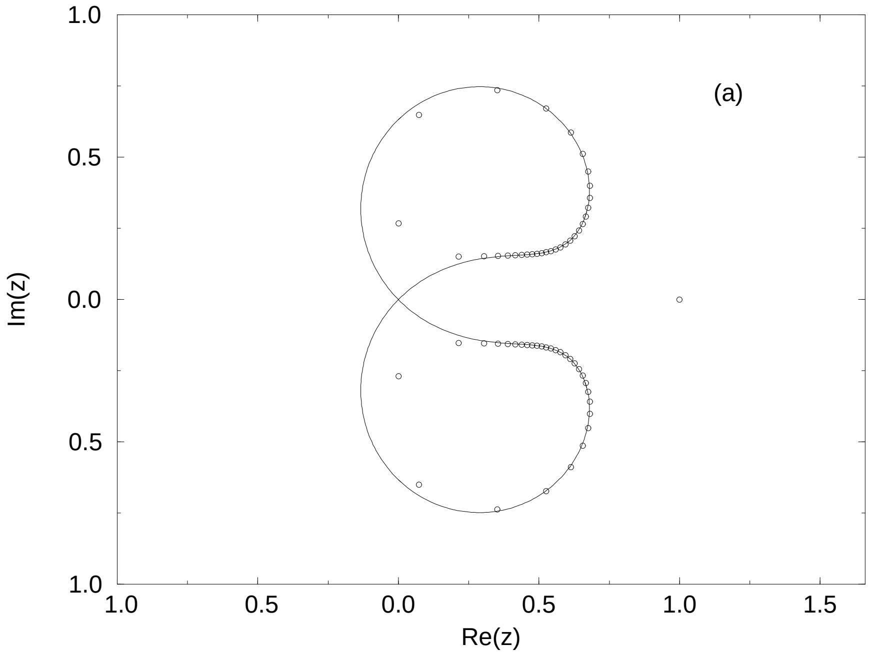

Figure 2. Boundary $\mathcal{B}$ in the $z = 1/q$-plane for $\lim_{r\to\infty} H_{k,r}$ with $k =$ (a) 4; (b) 5; (c) 6. Chromatic zeros for $H_{k,r}$ with (k, r) equal to (a) (4, 30); (b) (5, 18); (c) (6, 10) are shown for comparison.

As a further result, we find that (iii) if k is odd, $\mathcal{B}$ crosses the real q-axis once, at a value q_c that increases monotonically from $\frac{3}{2}$ for $k = 3$, with $\lim_{k\to\infty} q_c = 2$; (iv) if k is even, $\mathcal{B}$ never crosses the real q-axis, so q_c is not defined. To show these results, we first set $\beta = 0$ in equation (3.13), which becomes

$$(\rho + 1)^2\left[\rho^{k-2} + 2(-1)^k \sum_{s=0}^{k-3}(-\rho)^s\right] = 0. \tag{3.14}$$

For odd k, this has a single real, positive solution for ρ, which decreases monotonically from $\rho = 2$ for $k = 3$, approaching $\rho = 1$ as $k \to \infty$. For even k, equation (3.14) has no (real) solution for ρ. For $\beta = \pi$, equation (3.13) yields

$$(\rho - 1)^2\left[\rho^{k-2} + 2\sum_{s=0}^{k-3}\rho^s\right] = 0. \tag{3.15}$$

Aside from the root $\rho = 1$, i.e. $y = -1$, which is spurious as noted above, equation (3.15) has no real roots. The result for q follows directly.

The curves comprising $\mathcal{B}$ divide the z-(equivalently, y- or q-) plane into $k - 1$ regions. For even $k = 2\ell$ and odd $k = 2\ell + 1$, these include $(\ell - 1)$ c.c. pairs of regions. In the q-plane, $\mathcal{B}$ consists of $k - 2$ disjoint curves (a line for $k = 3$); each curve extends inward from complex infinity, turns around and heads back out to complex infinity along a different direction. For $k = 3$, $\mathcal{B}$ is a circle in both the y- and z-planes, given by the equation $|y-1| = 1$, i.e. $|z-\frac{1}{3}| = \frac{1}{3}$. For $k = 4, 5, 6$ we show our calculations of $\mathcal{B}$ in the z-planes in figure 2. The corresponding plots in the y-plane look more like (slightly distorted) cloverleafs, reflecting the simplicity of the degeneracy equation (3.11) in the y-variable. As

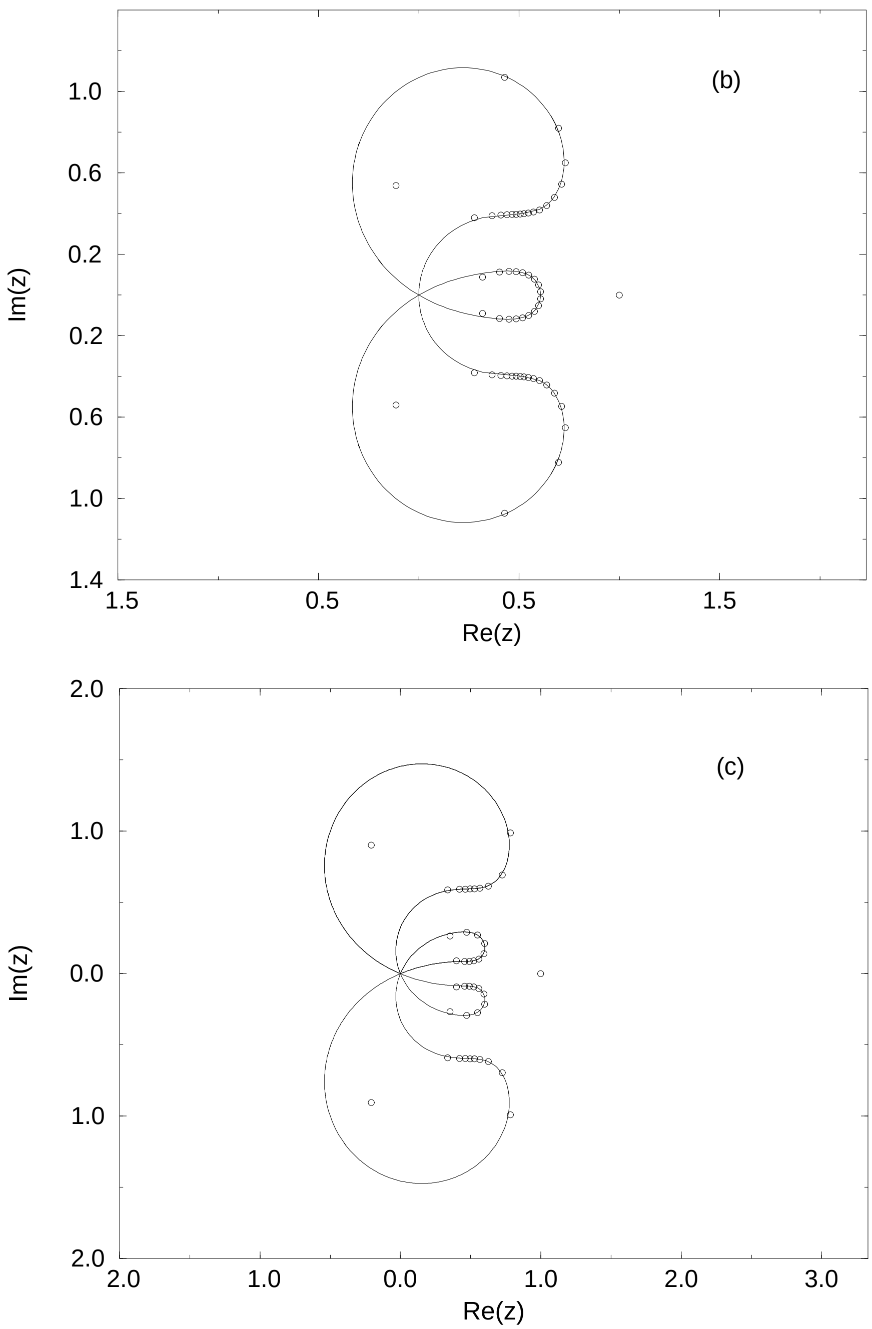

Figure 2. (Continued)

an example, we show the case $k = 6$ in figure 3 (additional figures in the y-plane are given in [21]). As is clear from figure 2, for $k \geqslant 4$, $\mathcal{B}$ has support for $\mathrm{Re}\,(q) < 0$ (equivalent to $\mathrm{Re}\,(z) < 0$). Note that $\mathrm{Re}\,(z) = 0$ does not, in general, imply that $z = 0$, since for $k \geqslant 4$,

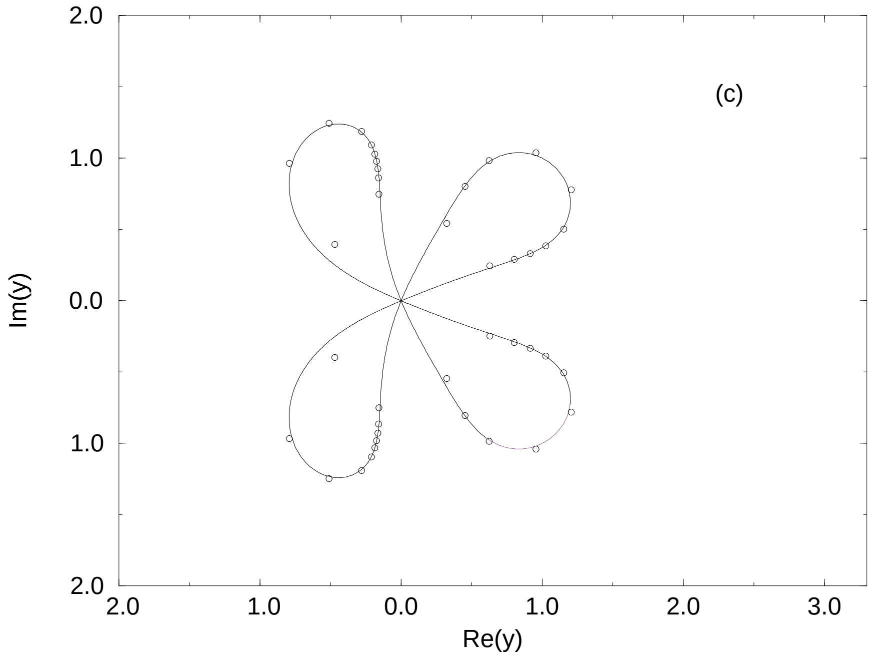

Figure 3. Boundary $\mathcal{B}$ in the $y = 1/(q-1)$-plane for $\lim_{r\to\infty} H_{k,r}$ with $k = 6$. Chromatic zeros for $H_{k,r}$ with $r = 10$ are shown for comparison.

$\mathcal{B}$ intersects the imaginary z-axis away from the origin, e.g. at $z = \pm z_i$, where

$$z_i = \mathrm{i}\sqrt{2/5} = 0.632\,456\mathrm{i} \qquad \text{for } k = 4 \tag{3.16}$$

$$z_i = \mathrm{i}\sqrt{8/7} = 1.069\,04\mathrm{i} \qquad \text{for } k = 5 \tag{3.17}$$

$$z_i = (\mathrm{i}/3)[10 \mp \sqrt{82}]^{1/2} = 0.323\,971\mathrm{i},\ 1.455\,08\mathrm{i} \qquad \text{for } k = 6. \tag{3.18}$$

In the y-plane, the intercepts $y = \pm\mathrm{i}\rho_i$ of $\mathcal{B}$ with the imaginary y-axis (aside from $y = 0$) are given, for even $k = 2\ell$, by

$$\rho_i^{2(\ell-1)}(\rho_i^2 - 1) - 2(-1)^\ell = 0 \tag{3.19}$$

and, for odd $k = 2\ell + 1$, by equation (3.19) multiplied by ρ. Solving these equations for general k, we find that (with $k > 3$) (i) for $k = (0 \text{ or } 1) \bmod 4$, ρ_i is nonzero, decreasing monotonically from $\sqrt{2}$ for $k = 4, 5$ toward 1 as $k \to \infty$; (ii) for $k = (2 \text{ or } 3) \bmod 4$, there is no nonzero intercept ρ_i. Although $\mathcal{B}$ extends to $\mathrm{Re}\,(z) < 0$ (equivalently, $\mathrm{Re}\,(q) < 0$), it never includes support for negative real z or q.

In figure 2 we also show illustrative chromatic zeros for (*a*) $k = 4$, $r = 30$ ($\Rightarrow n = 62$), (*b*) $k = 5$, $r = 18$ ($\Rightarrow n = 56$), and (*c*) $k = 6$, $r = 10$ ($\Rightarrow n = 42$). Aside from the ever-present zeros at $q = 0, 1$ ($z = \infty, 1$), the chromatic zeros generally lie close to the asymptotic curves comprising $\mathcal{B}$ onto which they coalesce as $k \to \infty$. For a given set of (finite) k and r, the moduli of the zeros are bounded, and hence they avoid the points $z = y = 0$, approaching these only as $r \to \infty$ for a given k.

As before [12, 13], we let R_1 denote the region including the positive real q-axis for $q > q_c$. For k even, this includes the entire real q-axis. For odd k, we denote the region containing the rest of the real q-axis as $R_{2,k\,\mathrm{odd}}$; from our statement above, it follows that there is no R_2 phase for k even. For $q \in R_1$, we calculate

$$W\Big(\Big[\lim_{r\to\infty} H_{k,r}\Big], q; q \in R_1\Big) = \begin{cases} [a_2(q)]^{1/(k-2)} & \text{if } k \text{ is odd} \\ [a_1(q)]^{1/(k-2)} & \text{if } k \text{ is even .} \end{cases} \tag{3.20}$$

As discussed in [12], in regions other than R_1, there is no canonical choice of phase in taking the $1/n$th root in equation (1.1), so that one can only determine $|W(\{G\}, q)|$. We find

$$\Big|W\Big(\Big[\lim_{r\to\infty} H_{k,r}\Big], q\Big)\Big| = |a_1(q)|^{1/(k-2)} \qquad \text{for } k \text{ odd and } q \in R_{2,k\,\text{odd}} \tag{3.21}$$

$$\Big|W\Big(\Big[\lim_{r\to\infty} H_{k,r}\Big], q\Big)\Big| = |a_2(q)|^{1/(k-2)} \qquad \text{for } k \text{ odd and } q \notin R_1, R_{2,k\,\text{odd}} \text{ and for } k \text{ even and } q \notin R_1. \tag{3.22}$$

On $\mathcal{B}$, $|W|$ is continuous but nonanalytic.

4. Class of families $HEC_{k_1-2,0,0}(\overline{K}_3 + \overline{K}_r)$

When $p \geqslant 3$ in the homeomorphic class of families (2.2) or (2.6) with $G_r = \overline{K}_r$, the graphs and their chromatic polynomials depend on the individual values of the k_j, not just on the sum, as in equation (3.1). A simple homeomorphic class of families of this type is the special case of equation (2.21) for $p = 3$ and $G_r = \overline{K}_r$, namely

$$\Theta_{k,r} = HEC_{k_1-2,0,0}(\overline{K}_3 + \overline{K}_r) \qquad k_1 \equiv k. \tag{4.1}$$

We have $v(\Theta_{k,r}) = r(k-1) + 3$ and

$$\chi(\Theta_{k,r}) = 2. \tag{4.2}$$

For our present purposes, it will suffice to study the family $\Theta_{3,r}$. We calculate the chromatic polynomial

$$\begin{aligned} P(\Theta_{3,r}, q) = {} & (q-2)^{2r-4} P(\Theta_{3,2}, q) - q(q-1)(D_4)^2[(q-2)^{2r-4} - (D_4)^{r-2}] \\ & - q(q-1)^2(q-2)^r[(q-2)^{r-2} - (q-1)^{r-2}] \\ & - q(q-1)(q-2)(q^2-4q+5)^2[(q-2)^{2r-4} - (q^2-4q+5)^{r-2}] \end{aligned} \tag{4.3}$$

where

$$P(\Theta_{3,2}, q) = q(q-1)[(q-1)D_6 - (q-2)D_5]. \tag{4.4}$$

This has the form of equation (1.2) with $N_a = 4$ and

$$a_1 = D_4 = q^2 - 3q + 3 \tag{4.5}$$

$$a_2 = q^2 - 4q + 5 \tag{4.6}$$

$$a_3 = (q-1)(q-2) \tag{4.7}$$

and

$$a_4 = (q-2)^2. \tag{4.8}$$

The nonanalytic boundary $\mathcal{B}$ for the limit as $r \to \infty$ is shown in figure 4. As with the $H_{k,r}$ family discussed above, and the other families to be discussed below, one sees the important feature that $\mathcal{B}$ includes support for $\mathrm{Re}\,(z) < 0$ or equivalently $\mathrm{Re}\,(q) < 0$. The boundary divides the z-(or equivalently y- or q-) plane into six different regions: (i) R_1, including the interval $0 < z < \frac{1}{2}$ on the positive real z-axis; (ii) R_2, including the union of the intervals $z > \frac{1}{2}$ and $z < 0$; (iii) a c.c. pair of regions R_3 and R_3^* lying just above and

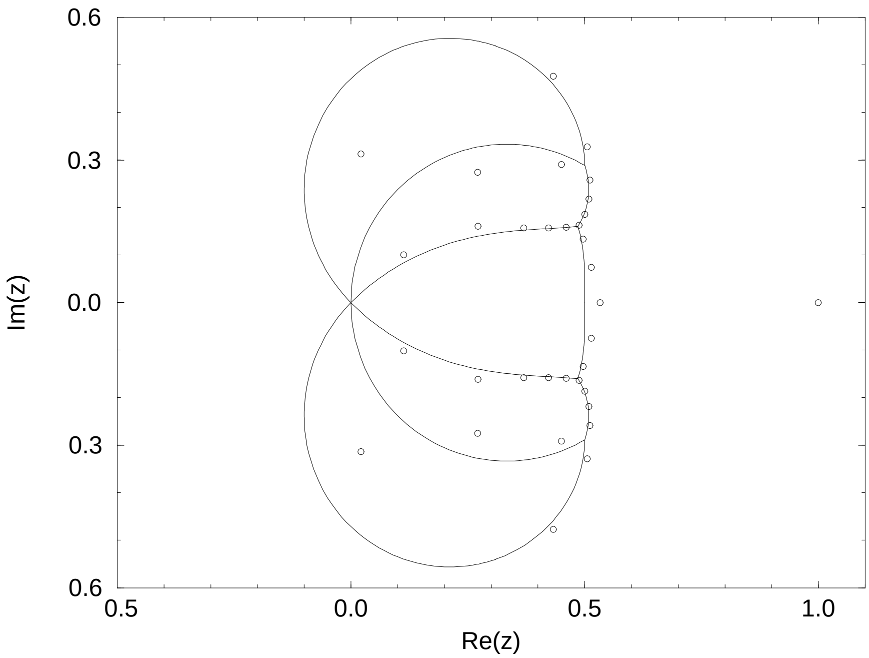

Figure 4. Boundary $\mathcal{B}$ in the $z = 1/q$-plane for $\lim_{r\to\infty} \Theta_{3,r}$. Chromatic zeros for $\Theta_{3,r}$ with $r = 16$ are shown for comparison.

below R_1 in the z-plane; and (iv) a second pair of c.c. regions R_4 and R_4^* located such that R_4 lies above and adjacent to R_3 (hence between R_3 and R_2) and R_4^* lies below R_3^*. In the regions R_1 and R_2, a_1 and a_2 are dominant, respectively, while a_j is dominant in regions R_j and R_j^* for $j = 3$ and $j = 4$, respectively. We have

$$W\Big(\Big[\lim_{r\to\infty} \Theta_{k,r}\Big], q\Big) = (a_1)^{1/2} \qquad \text{for } q \in R_1 \tag{4.9}$$

$$\Big|W\Big(\Big[\lim_{r\to\infty} \Theta_{k,r}\Big], q\Big)\Big| = |a_2|^{1/2} \qquad \text{for } q \in R_2 \tag{4.10}$$

and

$$\Big|W\Big(\Big[\lim_{r\to\infty} \Theta_{k,r}\Big], q\Big)\Big| = |a_j|^{1/2} \qquad \text{for } q \in R_j,\, R_j^*, \quad j = 3, 4. \tag{4.11}$$

The region boundaries between regions R_i and R_j are the solutions of the respective degeneracy equation $|a_i| = |a_j|$ where a_i and a_j are leading terms. Dividing these equations by $|q|^2$ and re-expressing them in terms of z to get the corresponding degeneracy equations in the z-plane, one has $|\tilde{a}_i| = |\tilde{a}_j|$ with $\tilde{a}_1 = 1-3z+3z^2$, $\tilde{a}_2 = 1-4z+5z^2$, $\tilde{a}_3 = (1-z)(1-2z)$, and $\tilde{a}_4 = (1-2z)^2$. Clearly, each (i, j) pair of the degeneracy equations $|\tilde{a}_i| = |\tilde{a}_j|$ in the z-plane has a solution at $z = 0$, which shows that, in accordance with the condition of [13], $\mathcal{B}$ is noncompact in the q-plane, passing through the point $z = 0$. Thus, as is evident in figure 4, all of the regions are contiguous at $z = 0$, where six curves (i.e. three branches) of $\mathcal{B}$ meet in a multiple point. For small $\zeta = |z|$, the degeneracy equation for the part of $\mathcal{B}$ separating R_1 and R_3 has the form $2\zeta^2(1 - 2\cos^2\theta) + O(\zeta^3) = 0$, so that this boundary crosses the point $z = 0$ at the angles given by $\cos\theta = 1/\sqrt{2}$, i.e.

$$\theta_{R_1,R_3}, \theta_{R_1,R_3^*} = \pm\frac{\pi}{4}. \tag{4.12}$$

(The other solution, $\cos\theta = -1/\sqrt{2}$ is not relevant because in this region, a_1 and a_3 are not leading terms.) Similarly, for small ζ, the degeneracy equation for the part of $\mathcal{B}$ separating the regions R_3 and R_4 is $\zeta(3\zeta - 2\cos\theta) = 0$ so that as $\zeta \to 0$, this boundary crosses the point $z = 0$ at the angles given by $\cos\theta = 0$, i.e.

$$\theta_{R_3,R_4}, \theta_{R_3^*,R_4^*} = \pm\frac{\pi}{2}. \tag{4.13}$$

The same type of reasoning applied to the R_2, R_4 and R_2, R_4^* boundaries shows that they cross $z = 0$ at the angles

$$\theta_{R_2,R_4}, \theta_{R_2,R_4^*} = \pm\frac{3\pi}{4}. \tag{4.14}$$

Concerning the boundary separating regions R_1 and R_2, we observe that the relevant degeneracy equation

$$\mathcal{B}(R_1 - R_2) : |1 - 3z + 3z^2| = |1 - 4z + 5z^2| \tag{4.15}$$

has the solution $z = \frac{1}{2}$ as its only solution other than $z = 0$ where a_1 and a_2 are leading terms. Hence, $q_c = 2$ for this family. Concerning the two c.c. pairs of multiple points, we note that the multiple point $z_{2,3,4}$ where regions R_2, R_3, and R_4 are contiguous, and its c.c., are

$$z_{2,3,4}, z_{2,3,4}^* = 3^{-1/2}\mathrm{e}^{\pm \mathrm{i}\pi/6} = \frac{1}{2} \pm \frac{\mathrm{i}}{2\sqrt{3}}. \tag{4.16}$$

Hence this c.c. pair lies on the unit circle $|y| = 1$ or equivalently $|q - 1| = 1$ in the respective y- and q-planes:

$$y_{2,3,4}, y_{2,3,4}^* = \mathrm{e}^{\pm \mathrm{i}\pi/3} \tag{4.17}$$

$$q_{2,3,4}, q_{2,3,4}^* = 3^{1/2}\mathrm{e}^{\pm \mathrm{i}\pi/6}. \tag{4.18}$$

A corresponding analysis can be given for the multiple point $z_{1,2,3}$ where regions R_1, R_2, and R_3 are contiguous.

5. Class of families $HEC_{k_1-2,k_2-2}(\overline{K}_2 + T_r)$

Illustrative graphs of the family

$$HEC_{k_1-2,k_2-2}(\overline{K}_2 + T_r) \tag{5.1}$$

with $(k_1, k_2) = (3, 2)$ and $(k_1, k_2) = (3, 3)$ are shown in figures 1(c) and (d), respectively. From the general equation (2.8) with $G_r = T_r$ and $p = 2$, we have

$$v(HEC_{k_1-2,k_2-2}(\overline{K}_2 + T_r)) = 2 + r(k_1 + k_2 - 3). \tag{5.2}$$

The special case $k_1 = k_2 = 2$ is the family $\overline{K}_2 + T_r = (K_2)_{b=1} + T_r$ which we analysed in detail earlier [13] so we concentrate on the homeomorphic expansions of this starting family here, i.e. $k_1 \geqslant 3$ and/or $k_2 \geqslant 3$. In order to calculate the chromatic polynomial for the graphs in this homeomorphic class of families, we shall utilize a generating function method as we did in [16] for infinitely long, finite-width strip graphs of various lattices. The generating function Γ is a function of a symbolic variable x and yields the chromatic polynomials $P(HEC_{k_1-2,k_2-2}(\overline{K}_2 + T_r), q)$ via the Taylor series expansion around $x = 0$ according to

$$\Gamma(HEC_{k_1-2,k_2-2}(\overline{K}_2 + T_r), q, x) = \sum_{r=1}^{\infty} P(HEC_{k_1-2,k_2-2}(\overline{K}_2 + T_r), q)x^r. \tag{5.3}$$

The summation starts at $r = 1$ since this is the minimum value of r in this family. As in our earlier work [16], we find that Γ is a rational function of x and, separately, of q, of the form

$$\Gamma(HEC_{k_1-2,k_2-2}(\overline{K}_2 + T_r), q, x) = \frac{\mathcal{N}(HEC_{k_1-2,k_2-2}(\overline{K}_2 + T_r), q, x)}{\mathcal{D}(HEC_{k_1-2,k_2-2}(\overline{K}_2 + T_r), q, x)} \tag{5.4}$$

with

$$\mathcal{N}(HEC_{k_1-2,k_2-2}(\overline{K}_2 + T_r), q, x) = x \sum_{j=0}^{j_{\max}} A_j(q) x^j \tag{5.5}$$

(so that $\deg_x(\mathcal{N}) = j_{\max} + 1$; the prefactor of x reflects the fact that the minimum value of r is 1) and

$$\mathcal{D}(HEC_{k_1-2,k_2-2}(\overline{K}_2 + T_r), q, x) = 1 + \sum_{j'=1}^{j'_{\max}} b_{j'}(q) x^{j'} \tag{5.6}$$

where $j_{\max}$ and $j'_{\max}$ depend on the specific family, the A_j and $b_{j'}$ are polynomials in q, and their dependence on k_1 and k_2 is left implicit. (This notation follows that of [16] except that in equation (5.5), we use A rather than a to avoid confusion with the a_j functions in equation (1.2).) A general formula for A_0 is

$$A_0 = P(T_{k_1+k_2-1}, q) = q(q-1)^{k_1+k_2-2}. \tag{5.7}$$

The other A_j's and $b_{j'}$ polynomials will be given below for specific families.

For the starting family, $HEC_{0,0}(\overline{K}_2 + T_r) = \overline{K}_2 + T_r = (K_2)_{b=1} + T_r$, and indeed its generalization $(K_p)_b + T_r$, one has [13]

$$P((K_p)_b + T_r, q) = q^{(p+1)}[(q-p-1)^{r-1} + b(q-p)^{r-2}] \tag{5.8}$$

(recall the notation in equation (1.8)). The equivalent representation in terms of a generating function is obtained by noting that equation (5.8) has the form of equation (1.2) with $c_0 = 0$ and $N_a = 2$, i.e.

$$P((K_p)_b + T_r, q) = c_1(a_1)^r + c_2(a_2)^r \tag{5.9}$$

with

$$a_1 = q - p - 1 \qquad a_2 = q - p \tag{5.10}$$

$$c_1 = \frac{q^{(p+1)}}{q-p-1} \tag{5.11}$$

and

$$c_2 = \frac{bq^{(p+1)}}{(q-p)^2}. \tag{5.12}$$

We find that the chromatic polynomial $P((K_p)_b + T_r, q)$ is given as the coefficient of x^r in the Taylor series expansion about $x = 0$ of the generating function

$$\Gamma((K_p)_b + T_r, q; x) = \frac{x(A_0 + A_1 x)}{(1-\lambda_1 x)(1-\lambda_2 x)} \tag{5.13}$$

where

$$\lambda_j = a_j \qquad j = 1, 2 \tag{5.14}$$

$$A_0 = a_1 c_1 + a_2 c_2 \tag{5.15}$$

and

$$A_1 = -a_1 a_2 (c_1 + c_2). \tag{5.16}$$

For a general graph G, this type of relation between the form for the chromatic polynomial (5.9) and the generating function (5.13) has a straightforward generalization to the case where $N_a \geqslant 3$. In the present case $(K_2)_{b=1} + T_r = HEC_{0,0}(\overline{K}_2 + T_r)$, we find, for the upper limits on the sums in $\mathcal{N}(x)$ and $\mathcal{D}(x)$ the values $j_{\max} = 1$ and $j'_{\max} = 2$.

5.1. Families $HEC_{k_1-2,0}(\overline{K}_2 + T_r)$

We first consider the simplest homeomorphic expansion of type HEC on the starting family $\overline{K}_2 + T_r$, in which one performs this expansion only on the bonds connecting one of the two vertices in the $\overline{K}_2$ subgraph with the vertices of the T_r subgraph. With no loss of generality, we choose this vertex in $\overline{K}_2$ to be v_1, so that $k_2 - 2 = 0$ and $k_1 - 2 \geqslant 1$. For brevity of notation, define

$$O_{k,r} = HEC_{k_1-2,0}(\overline{K}_2 + T_r) \qquad k_1 \equiv k \tag{5.17}$$

with $v(O_{k,r}) = 2 + r(k-1)$. When referring to the collection of the graphs of this family for various r, we denote it as $\{O_k\}$. The case $k = 2$ is just the original starting family, $\overline{K}_2 + T_r$. For the family $O_{k,r}$ with $k \geqslant 3$ we find that

$$j_{\max} = 2 \qquad j'_{\max} = 3. \tag{5.18}$$

For general $k \geqslant 3$, the denominator of the generating function can be written as

$$\begin{aligned} \mathcal{D}(\{O_k\}, q, x) &= [1 - (q-2)D_k x][1 - (q-3)D_k x - (q-1)(q-2)D_{k-1}D_k x^2] \\ &= (1 - \lambda_2 x)(1 - \lambda_{1p} x)(1 - \lambda_{1m} x) \end{aligned} \tag{5.19}$$

where

$$\lambda_{1p,m} = \tfrac{1}{2}[(q-3)D_k \pm [\{(q-3)D_k\}^2 + 4(q-1)(q-2)D_{k-1}D_k]^{1/2}] \tag{5.20}$$

and

$$\lambda_2 = (q-2)D_k. \tag{5.21}$$

The coefficient functions in $\mathcal{N}$ are A_0, given by the special case of equation (5.7), namely $A_0 = q(q-1)^k$, and

$$A_1 = -q(q-1)D_k[(2q-5)(q-1)^{k-1} - (q-2)[qD_k - 2(-1)^k]] \tag{5.22}$$

$$A_2 = -q^2(q-1)^2(q-2)D_{k-1}D_k^2. \tag{5.23}$$

(In deriving the expression for A_1, we have used the identity $D_{2k-1} = [qD_k - 2(-1)^k]D_k$.) We calculate

$$W(\{O_k\}, q) = (\lambda_{\max})^{1/(k-1)} \qquad \text{for } q \in R_1 \tag{5.24}$$

and

$$|W(\{O_k\}, q)| = |\lambda_{\max}|^{1/(k-1)} \qquad \text{for } q \in R_j \neq R_1 \tag{5.25}$$

where $\lambda_{\max}(q)$ denotes the leading λ in equation (5.19) in the respective regions of the q-plane. For a general family $\{G\}$ of graphs with a generating function

$$\Gamma(\{G\}, q, x) = \frac{\mathcal{N}(x)}{\mathcal{D}(x)} = \sum_{j=j_0}^{\infty} P(G_r, q) x^r \tag{5.26}$$

with

$$\mathcal{D}(x) = \prod_{j'=1}^{j'_{\max}} (1 - \lambda_j x) \tag{5.27}$$

the boundary $\mathcal{B}$ in the limit $r \to \infty$ is given (see equation (4.16) of the first paper in [16]) as solution locus of the equation expressing the degeneracy in magnitude of two leading λ terms in equation (5.27), where W switches form nonanalytically,

$$|\lambda_{\max}(q)| = |\lambda_{\max'}(q)|. \tag{5.28}$$

As an illustration, we consider the lowest homeomorphic expansion, $k = 3$, for which equations (5.20) and (5.21) read

$$\lambda_{1p,m} = \tfrac{1}{2}(q-2)[(q-3) \pm (q^2 - 2q + 5)^{1/2}] \tag{5.29}$$

$$\lambda_2 = (q-2)^2. \tag{5.30}$$

Let us now write λ_{1p}, λ_{1m} and λ_2 in terms of the variable $z = 1/q$ in polar coordinates, as given by equation (1.4) and Taylor-expand the resulting expressions for small ζ. We obtain for the magnitudes squared of the λ's

$$|\lambda_{1p}|^2 = 1 - 4\zeta\cos\theta + 2\zeta^2(\cos(2\theta) + 2) + \mathrm{O}(\zeta^3) \tag{5.31}$$

$$|\lambda_{1m}|^2 = \zeta^2 + \mathrm{O}(\zeta^3) \tag{5.32}$$

$$|\lambda_2|^2 = 1 - 4\zeta\cos\theta + 4\zeta^2 + \mathrm{O}(\zeta^3). \tag{5.33}$$

Thus, for small values of $|z|$, the boundary $\mathcal{B}$ is given by the equation $|\lambda_{1p}| = |\lambda_2|$, which yields $\zeta^2\cos(2\theta) + \mathrm{O}(\zeta^3) = 0$ as $\zeta \to 0$. Hence, $\mathcal{B}$ is noncompact in the q-plane and crosses the origin of the z-plane at angles such that $\cos(2\theta) = 0$, i.e.

$$\theta = \frac{\pi}{4} + n\frac{\pi}{2} \qquad 0 \leqslant n \leqslant 3. \tag{5.34}$$

This is evident in figure 5. From equation (1.3), it follows that $y \to z$ as $z \to 0$, so that these angles are the same in the y-plane. The boundary $\mathcal{B}$ divides the z-plane into four regions: (i) R_1, including the interval $0 < z < \frac{1}{3}$ on the real z-axis; (ii) R_2, including the intervals $-\infty < z < 0$ and $\frac{1}{3} < z < \infty$ on the real z-axis; and (iii) the complex-conjugate pair of regions R_3 and R_3^* lying roughly above and below $z = 0$.

We find

$$W\Big(\Big[\lim_{r\to\infty} O_{3,r}\Big], q\Big) = (\lambda_{1p})^{1/2} \qquad \text{for } q \in R_1 \tag{5.35}$$

$$\Big|W\Big(\Big[\lim_{r\to\infty} O_{3,r}\Big], q\Big)\Big| = |\lambda_{1p}|^{1/2} \qquad \text{for } q \in R_2 \tag{5.36}$$

and

$$\Big|W\Big(\Big[\lim_{r\to\infty} O_{3,r}\Big], q\Big)\Big| = |\lambda_2|^{1/2} \qquad \text{for } q \in R_3, R_3^*. \tag{5.37}$$

A portion of $\mathcal{B}$ crosses the positive real axis at $z = z_c = \frac{1}{3}$ so that $q_c = 3$ for $\lim_{r\to\infty} O_{3,r}$. Along this portion of the boundary $|\lambda_{1m}|$ becomes degenerate with $|\lambda_{1p}|$, although the former never dominates in magnitude over the latter. This portion of the boundary ends in two c.c. multiple points. Note that

$$W\Big(\Big[\lim_{r\to\infty} O_{3,r}\Big], q\Big) = 0 \qquad \text{at } q = 2 \tag{5.38}$$

consistent with equations (2.11) and (2.12).

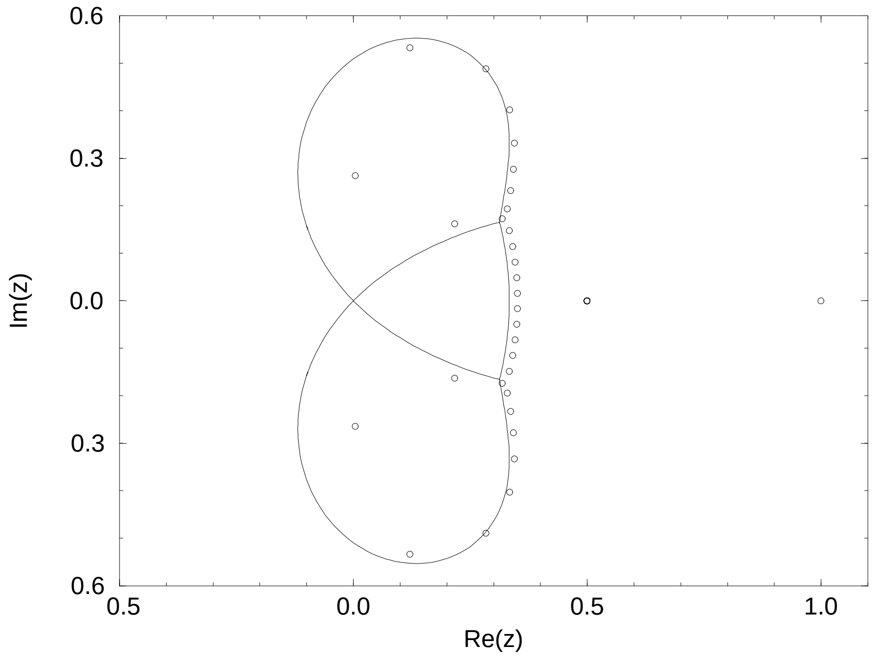

Figure 5. Boundary $\mathcal{B}$ in the $z = 1/q$-plane for $\lim_{r\to\infty} O_{k,r}$ with $k = 3$. Chromatic zeros for $O_{k,r}$ $(k, r) = (3, 29)$ are shown for comparison.

5.2. Families $HEC_{k_1-2,k_2-2}(\overline{K}_2 + T_r)$ with $k_1 = k_2$

We next consider the case of symmetric homeomorphic expansion of the bonds from the two vertices of the $\overline{K}_2$ subgraph, i.e. $k_1 = k_2 \equiv k$. For brevity of notation, we denote

$$U_{k,r} = HEC_{k_1-2,k_2-2}(\overline{K}_2 + T_r) \qquad k_1 = k_2 \equiv k \tag{5.39}$$

with $v(U_{k,r}) = 2 + r(2k - 3)$. When referring to the collection of the graphs of this family for various r, we denote it as $\{U_k\}$.

For the family $U_{k,r}$ we find that

$$j_{\max} = 3 \qquad j'_{\max} = 4. \tag{5.40}$$

The denominator of the generating function can be written as

$$\mathcal{D}(\{U_k\}, q, x) = [1 - (q-2)D_k^2 x - (q-1)^3 D_{k-1}^2 D_k^2 x^2] \\ \times [1 - D_k(D_{k+1} - D_k)x - (q-1)^2 D_{k-1} D_k^3 x^2]. \tag{5.41}$$

Observe that each factor of x in $\mathcal{D}(\{U_k\}, q, x)$ occurs with at least one accompanying factor of D_k. We have

$$\mathcal{D}(\{U_k\}, q, x) = (1 - \lambda_{1p}x)(1 - \lambda_{1m}x)(1 - \lambda_{2p}x)(1 - \lambda_{2m}x) \tag{5.42}$$

where

$$\lambda_{1p,m} = \frac{D_k}{2}[(q-2)D_k \pm [[(q-2)D_k]^2 + 4(q-1)^3(D_{k-1})^2]^{1/2}] \tag{5.43}$$

and

$$\lambda_{2p,m} = \frac{D_k}{2}[(D_{k+1} - D_k) \pm [(D_{k+1} - D_k)^2 + 4(q-1)^2 D_{k-1} D_k]^{1/2}]. \tag{5.44}$$

For the polynomials in the numerator $\mathcal{N}(x)$, equation (5.7) gives $A_0 = q(q-1)^{2k-2}$ and we find

$$A_1 = q(q-1)[(D_{2k-1})^2 - (q-1)^{2k-3}[(q-3)D_k + D_{k+1}]D_k] \tag{5.45}$$

$$A_2 = -q(q-1)^2 D_{k-1} D_k^3 [q^2 D_k^2 - q(q+2)(-1)^k D_k + 2q + q(q-2)(q-1)^{k-2} D_k + (q-2)(-1)^k (q-1)^{k-2} + 1] \tag{5.46}$$

$$A_3 = -q^3 (q-1)^4 D_{k-1}^3 D_k^5. \tag{5.47}$$

We calculate

$$W(\{U_k\}, q) = [\lambda_{\max}(q)]^{1/(2k-3)} \qquad \text{for } q \in R_1 \tag{5.48}$$

and

$$|W(\{U_k\}, q)| = |\lambda_{\max}(q)|^{1/(2k-3)} \qquad \text{for } q \in R_j \neq R_1 \tag{5.49}$$

where $\lambda_{\max}(q)$ refers to the respective dominant λ in the given region. The boundary $\mathcal{B}$ is given, as before, by the solution locus of equation (5.28). We show this boundary in figure 6(a), together with illustrative chromatic zeros for the case $r = 19$. From the property (2.15), it follows that the λ's are degenerate at zero when $q = 2$,

$$\lambda_{1p,m}(q=2) = \lambda_{2p,m}(q=2) = 0 \qquad \text{for } k \text{ odd} \tag{5.50}$$

so that $\mathcal{B}$ passes through the point $q = 2$ if k is odd, and, furthermore,

$$W\left(\left[\lim_{r\to\infty} U_{k,r}\right], q=2\right) = 0 \qquad \text{for } k \text{ odd.} \tag{5.51}$$

This is consistent with the facts that $\chi(\{U_k\}) = 3$ and $P(U_{k,r}, q=2) = 0$ as special cases of equations (2.11) and (2.12).

We next give some explicit results for the lowest two cases, $k = 3$ and $k = 4$. For the family $U_{k=3,r}$ equations (5.43) and (5.44) yield

$$\lambda_{1p,m;k=3} = \tfrac{1}{2}(q-2)[(q-2)^2 \pm (q^4 - 4q^3 + 12q^2 - 20q + 12)^{1/2}] \tag{5.52}$$

$$\lambda_{2p,m;k=3} = \tfrac{1}{2}(q-2)[(q^2 - 4q + 5) \pm (q^4 - 4q^3 + 10q^2 - 20q + 17)^{1/2}]. \tag{5.53}$$

To investigate the boundary in the vicinity of $z = 0$, we divide the degeneracy equations by $|q|^3$ and express the results in terms of $z = 1/q$ in polar coordinates, as given by equation (1.4). We then Taylor-expand these equations for small $\zeta = |z|$. This yields

$$|\lambda_{1p;k=3}|^2 = 4 - 24\zeta\cos\theta + 4\zeta^2[8\cos(2\theta) + 9] - 8\zeta^3[12\cos\theta + \cos(3\theta)] + \mathrm{O}(\zeta^4) \tag{5.54}$$

$$|\lambda_{2p;k=3}|^2 = 4 - 24\zeta\cos\theta + 4\zeta^2[8\cos(2\theta) + 9] - 16\zeta^3[6\cos\theta + \cos(3\theta)] + \mathrm{O}(\zeta^4) \tag{5.55}$$

$$|\lambda_{1m;k=3}|^2 = 4\zeta^2 + \mathrm{O}(\zeta^3) \tag{5.56}$$

$$|\lambda_{2m;k=3}|^2 = 4\zeta^2 + \mathrm{O}(\zeta^3). \tag{5.57}$$

Thus, in the vicinity of $z = 0$ the boundary $\mathcal{B}$ is given by the equation $|\lambda_{1p;k=3}| = |\lambda_{2p;k=3}|$, which yields $\cos(3\theta) = 0$ for $\zeta \neq 0$. Hence, six curves on $\mathcal{B}$ (forming three branches) cross the point $z = 0$ (and hence also the point $y = 0$), at angles

$$\theta = \frac{\pi}{6} + n\frac{\pi}{3} \qquad 0 \leqslant n \leqslant 5. \tag{5.58}$$

The boundary $\mathcal{B}$ divides the z-plane into six regions. As one traverses a circle around the origin, $z = 0$, starting with a small positive real z-value, first $\lambda_{1p;k=3}$ is dominant, and then the dominant λ's alternate between $\lambda_{1p;k=3}$ and $\lambda_{2p;k=3}$. The resultant W-functions are given by equations (5.48) and (5.49).

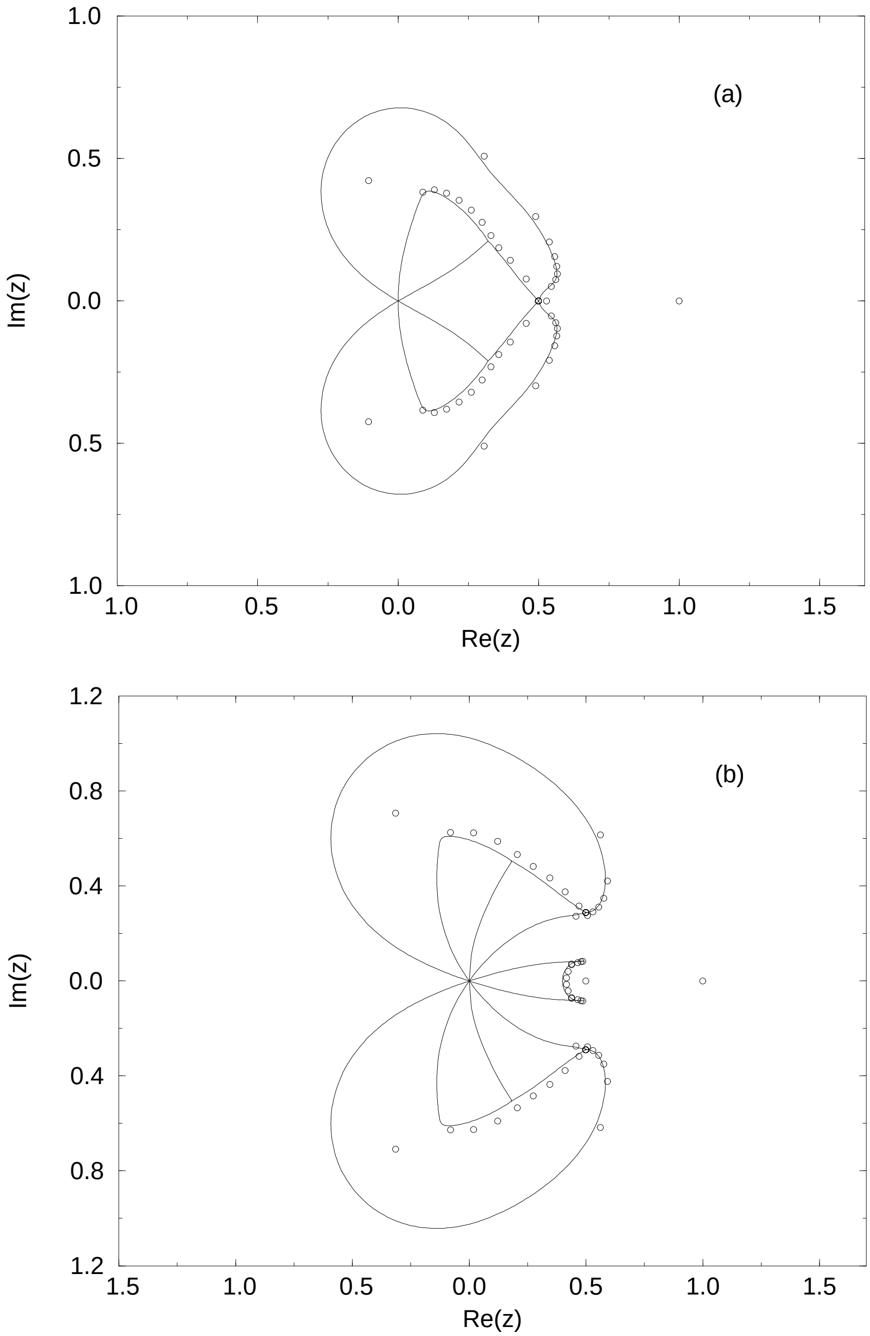

Figure 6. Boundary $\mathcal{B}$ in the $z = 1/q$-plane for $\lim_{r\to\infty} U_{k,r}$ with k equal to (a) 3; (b) 4. Chromatic zeros for $U_{k,r}$ with (k, r) equal to (a) (3,19); (b) (4,15) are shown for comparison.

For the family $U_{k=4,r}$ equations (5.43) and (5.44) yield

$$\lambda_{1p,m;k=4} = \tfrac{1}{2}(q-2)(q^2-3q+3)[(q^2-3q+3) \pm (q^4-2q^3+3q^2-6q+5)^{1/2}] \quad (5.59)$$

$$\lambda_{2p,m;k=4} = \frac{1}{2}(q^2-3q+3)[(q^3-5q^2+9q-7) \pm(q^6-6q^5+15q^4-24q^3+35q^2-42q+25)^{1/2}]. \tag{5.60}$$

As before, the boundary $\mathcal{B}$ is determined by equation (5.28). This boundary is plotted in figure 6(*b*). Let us write $\lambda_{1p,m}$ and $\lambda_{2p,m}$ in terms of the variable $z = 1/q$ in polar coordinates, as given by equation (1.4) and Taylor-expand the resulting expressions for small ζ. We find that the two λ's that are dominant near $z = 0$, namely λ_{1p} and λ_{2p}, have squared magnitudes that coincide through $\mathrm{O}(\zeta^4)$ and differ in $\mathrm{O}(\zeta^5)$ in the coefficient of $\zeta^5\cos(5\theta)$. (The other two λ's are subdominant near $z = 0$; indeed, they vanish there, as $|\lambda_{1m}|^2 \sim |\lambda_{2m}|^2 = 4\zeta^2 + \mathrm{O}(\zeta^3)$.) It follows that as $\zeta \to 0$, the boundary $\mathcal{B}$ is given by the equation $|\lambda_{1p}| = |\lambda_{2p}|$, which yields $\cos(5\theta) = 0$ for $\zeta \neq 0$. Hence, 10 curves, forming five branches of $\mathcal{B}$, cross the point $z = 0$ (and also $y = 0$) at the angles

$$\theta = \frac{\pi}{10} + n\frac{\pi}{5} \qquad 0 \leqslant n \leqslant 9. \tag{5.61}$$

Here, the boundary $\mathcal{B}$ divides the z-plane into eight regions. As one traverses a circle around the origin starting with a small positive real value of z, first $\lambda_{1p;k=4}$ is dominant, and then the dominant λ's alternate between $\lambda_{1p;k=4}$ and $\lambda_{2p;k=4}$, as before with $k = 3$. The resultant W-functions again follow from eqs. (5.48) and (5.49). Thus, comparing our results for $U_{k,r}$ with $k = 3$ and $k = 4$, we observe that the number of curves on $\mathcal{B}$ passing through $z = 0$, and the number of regions, increase as k is increased. One should also remark that certain properties of the region depend on whether k is even or odd, such as the fact that $\mathcal{B}$ passes through $z = \frac{1}{2}$ for odd $k \geqslant 3$.

6. Discussion

In this section we discuss general features of the Potts antiferromagnet W-functions on all of the families of graphs that we have constructed and studied in this paper and our earlier work, with loci $\mathcal{B}$ that are noncompact in the q-plane. In the theorem of section 4 of [13] we gave the general algebraic condition that for a particular family of graphs, the infinite-vertex limit yields a locus $\mathcal{B}$ that passes through $z = 0$. From our calculations we have observed a geometrical regularity in the families of graphs that have this property, namely that in this infinite-vertex limit they all contain an infinite number of different, nonoverlapping (and nonself-intersecting) circuits, each of which passes through at least two fixed, nonadjacent vertices. This immediately implies that these aforementioned nonadjacent vertices have degrees Δ that go to infinity in this limit. One thus sees at the graphical level why the derivation of the large-q series for the reduced function $W_{\mathrm{red}}(\{G\}, q)$ or equivalently $\overline{W}(\{G\}, q)$ on regular lattices with free or some type of periodic boundary conditions works; in the thermodynamic limit, such lattices do not have the two or more nonadjacent vertices with degrees $\Delta \to \infty$ as in the criterion stated above for noncompact $\mathcal{B}$.

We remark that in studies of the Potts model on regular lattices, it has been useful to utilize certain boundary conditions that do involve vertices which, in the thermodynamic limit, have infinite degree Δ, since these make it possible to preserve exact duality on finite lattices [23–25]. On the square lattice, the duality-preserving boundary conditions (DBCs) of types DBC-1 and DBC-2, in the notation of [25] involve one such vertex with $\Delta \to \infty$ while the DBC-3 type involves two such vertices; however, in the latter case, these are adjacent. Hence, none of these duality-preserving boundary conditions invalidates a large-q expansion of $W_{\mathrm{red}}(\{G\}, q)$ for this lattice.

An elementary topological property should be noted: for an arbitrary family of graphs, the continuous locus of points $\mathcal{B}$ where W is nonanalytic in the infinite-vertex limit does not necessarily enclose regions in the q-plane. Indeed, in [16] we carried out exact calculations of a variety of infinitely long, finite-width strips of different lattices and found loci $\mathcal{B}$ that consisted of arcs (and line segments) that did not enclose regions. (We have also performed similar calculations for other types of strips with specific types of end-graphs that yield loci $\mathcal{B}$ that do enclose regions.) None of these loci were noncompact in the q-plane. In contrast, if the infinite-vertex limit of a family of graphs yields a locus $\mathcal{B}$ that passes through $z = 0$, then, given that it is not a semi-infinite line segment on the positive or negative z-plane, it necessarily separates the z- and equivalently the q- or y-planes into at least two different regions where W is an analytic function. In [16] we observed that the endpoints of the arcs (or line segments on the real q-axis) that comprised the nonanalytic locus $\mathcal{B}$ were determined by the branch points of certain algebraic expressions occurring in the λ's that entered in degeneracy equations of the form of equation (5.28). Since, for example, the λ's for the family $\{U_k\}$, equations (5.43) and (5.44), also contain square roots, one may wonder what role the branch points of these roots play with regard to the boundary $\mathcal{B}$. We have investigated this and have found that the analogues of the arcs extending between branch points of the square roots, which comprised the various boundaries in [16], do not yield endpoint singularities on $\mathcal{B}$ here. The reason for this is that either (i) these arcs involve degeneracy of λ's that are nonleading in a given region, or (ii) although they coincide on part of their length with the actual boundary, the portion of the arcs containing the endpoints lies off this boundary, in a region where condition (i) holds. This is illustrated in figure 7 for the $\{U_k\}$ family with $k = 3$, where we show the actual boundary $\mathcal{B}$, as in figure 6(a), together with the arcs (drawn in a thicker black) formed by the degeneracy conditions

$$|\lambda_{2p}| = |\lambda_{2m}| \tag{6.1}$$

and

$$|\lambda_{1p}| = |\lambda_{1m}|. \tag{6.2}$$

The c.c. pair of arcs which constitute the solution locus to equation (6.1), with endpoints at $z_{2a}, z_{2a}^* = 0.041\,06 \pm 0.436\,27\mathrm{i}$ and $z_{2b}, z_{2b}^* = 0.547\,17 \pm 0.083\,33\mathrm{i}$, lie in the interior of the regions R_4 and R_4^*. But in these regions, neither λ_{2p} nor λ_{2m} is dominant; rather, as we discussed in the section on the $U_{k,r}$ family, it is λ_{1p} that is dominant in these regions. Hence, this c.c. pair of arcs is not relevant to the actual boundary. As shown in figure 7, the locus of solutions for the degeneracy equation (6.2) forms a c.c. pair of arcs that cross each other and the real z-axis at $z = \frac{1}{2}$ and have endpoints at $z_{1a}, z_{1a}^* = 0.101\,69 \pm 0.375\,29\mathrm{i}$ and $z_{1b}, z_{1b}^* = 0.731\,64 \pm 0.126\,12\mathrm{i}$. The portion of these arcs that lie to the right of $\mathrm{Re}\,(z) = \frac{1}{2}$ are not relevant for determining the boundary because in this region, denoted R_2 in our section above on the $\{U_k\}$ family, the dominant λ is λ_{2p}. The portion of the c.c. arcs lying between the multiple (crossing) point $z = \frac{1}{2}$ on the right and the multiple points forming T-intersections on the left at $z_T, z_T^* = 0.3204 \pm 0.2110\mathrm{i}$ does coincide with the boundary, since on this portion the boundary is determined by the degeneracy of magnitudes of leading eigenvalues λ_{1p} and λ_{1m}, i.e. equation (6.2). However, to the left of these T-intersection points, the arcs forming the solution locus of equation (6.2) again deviate from the actual boundary, which is determined by the degeneracy of leading magnitudes $|\lambda_{2p}| = |\lambda_{1p}|$. Hence, once again, the left endpoints of these arcs are not relevant for $\mathcal{B}$. Thus, the boundaries $\mathcal{B}$ for the families considered here, even aside from the fact that they automatically enclose regions owing to their noncompactness, in contrast to the arcs comprising the loci $\mathcal{B}$ for the strip graphs that we studied in [16], also differ qualitatively in that they do not contain any arc endpoints. We have explained why this is so even though some of the families do have λ's containing branch points singularities.

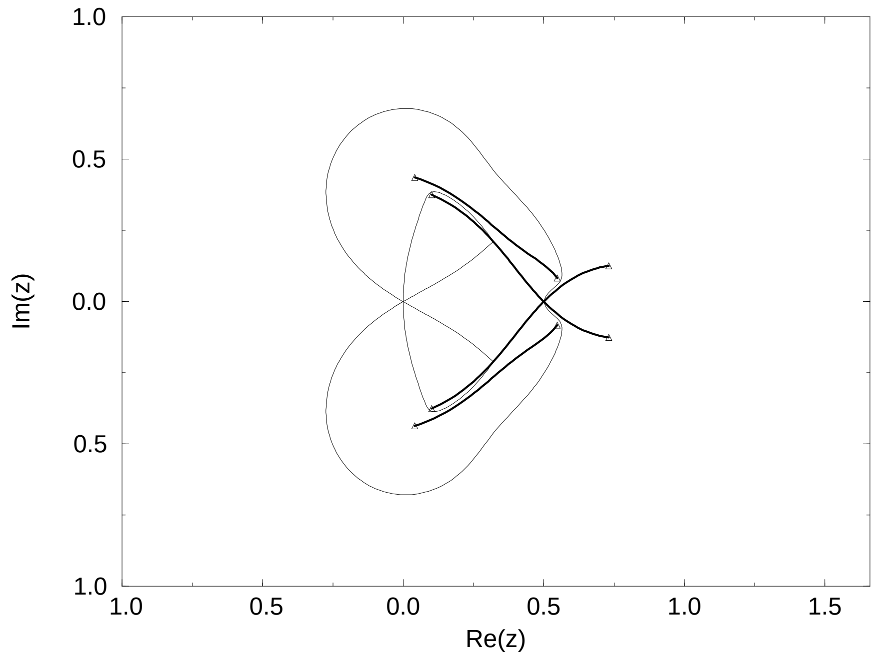

Figure 7. Boundary $\mathcal{B}$ in the $z = 1/q$-plane for $\lim_{r\to\infty} U_{3,r}$, shown together with the locus of solutions of the degeneracy equations (6.1) and (6.2). See text for discussion.

This emphasizes that the existence of the arc-like structure of the loci $\mathcal{B}$ that we found in [16] depended not just on the presence of branch point singularities in the λ's entering via equations analogous to equation (5.42) in the denominators $\mathcal{D}$ of the generating functions for various strip graphs, but also on the fact that these branch point singularities occurred at endpoints of arcs in regions where these arcs were the solution loci of magnitude degeneracy equations for leading λ's.

From our studies of many homeomorphic expansions, we have found the general feature that for a given homeomorphic class parametrized by some set of homeomorphic expansion indices $\{k_j\}$, the number of regions separated by the locus $\mathcal{B}$ in the $r \to \infty$ limit is a nondecreasing function of the above expansion indices. This is in accord with the constraints from algebraic geometry, in particular, the Harnack theorem [20]. The application of this theorem is simplest in the case where $\mathcal{B}$ is a nonsingular algebraic curve (so that the number of regions $N_{\rm reg} = N_{\rm comp} + 1$ where $N_{\rm comp}$ denotes the number of connected components of $\mathcal{B}$), as is the case for the $r \to \infty$ limit of the families $T_{k,r} = HEG_{k-2}(\overline{K}_2 + T_r)$ and $S_{k,r} = HEG_{k-2}(\overline{K}_3 + T_r)$ [26]. In these cases (where $\mathcal{B}$ has no multiple points) the Harnack theorem states that the number of regions is bounded above by $g + 1$, where g is the genus of the algebraic equation in the variables $\mathrm{Re}\,(q)$ and $\mathrm{Im}\,(q)$ whose solution set is $\mathcal{B}$, namely $g = (d-1)(d-2)/2$ where d is the homogeneous degree of this equation. Since, as our exact solutions show, this degree and the resultant genus increase as a function of the homeomorphic expansion indices, the Harnack upper bound also increases. It should be noted, however, that the number of regions may remain the same as one performs a homeomorphic expansion (e.g. $N_{\rm reg} = 2$ for the $r \to \infty$ limit of $HEG_{k-2}(\overline{K}_2 + T_r)$ for $k = 2, 3$, and 4, then $N_{\rm reg} = 3$ for $k = 5, 6$, and 7, etc).

For algebraic curves $\mathcal{B}$ with singularities such as multiple points, one no longer has the simple relation $N_{\rm reg} = N_{\rm comp} + 1$. Indeed, in the families constructed and analysed in this paper, $\mathcal{B}$ consists of a single connected component, i.e. $N_{\rm comp} = 1$, while the number of regions $N_{\rm reg}$ and the index of the multiple point at $z = 0$ increase as a function of the indices $\{k_j\}$ describing the homeomorphic expansions. The origin of this increase is the increase in the degree of the polynomials in z that occur in the degeneracy equations relevant for the boundary $\mathcal{B}$ in the neighbourhood of $z = 0$ (e.g. eqs. (3.11) and the resultant (3.12) for $H_{k,r}$, etc).

The boundaries $\mathcal{B}$ found for the families of graphs in this paper exhibit some interesting differences with respect to the (similarly noncompact) boundaries that we have previously studied [13]; the latter shared three general properties: (i) a single curve on $\mathcal{B}$ passes through $z = 0$, so that this point is a regular point on $\mathcal{B}$ as an algebraic curve; (ii) if $q \in \mathcal{B}$, then $\mathrm{Re}\,(q) \geqslant 0$, i.e. $\mathcal{B}$ includes support only for $\mathrm{Re}\,(q) \geqslant 0$, or equivalently, for $\mathrm{Re}\,(z) \geqslant 0$; and (iii) if $z \in \mathcal{B}$ and $\mathrm{Re}\,(z) = 0$, then $z = 0$. In contrast, for the families studied in the present paper, the homeomorphic expansions, which are all of the type HEC, yield, in the $r \to \infty$ limit, respective boundaries $\mathcal{B}$ that differ in each of these aspects: (i) several branches of the algebraic curve $\mathcal{B}$ pass through the point $z = 0$, which is thus a singular (multiple) point on this curve; (ii) $\mathcal{B}$ includes support for $\mathrm{Re}\,(q) < 0$ or equivalently $\mathrm{Re}\,(z) < 0$, and (iii) $\mathcal{B}$ includes points with $\mathrm{Re}\,(z) = 0$ other than $z = 0$ itself. Some insight into this can be gained by recalling the differences in the types of homeomorphic expansions of starting graphs. Since in the original starting families such as $(K_p)_b + G_r$ and $\overline{K}_p + G_r$, it was the connecting bonds linking the vertices of the K_p subgraph with the vertices of the G_r subgraph that gave rise to the noncompactness of the respective boundaries $\mathcal{B}$, it makes sense that homeomorphic expansions of these bonds would alter the nature of the boundaries at $z = 0$. Since this change involves multiple branches of $\mathcal{B}$ passing through this point at various angles, as in equations (3.12), (5.34), (5.58) and (5.61), this also shows why this type of homeomorphic expansion leads to boundaries that include support for $\mathrm{Re}\,(q) < 0$, but $q \neq 0, \infty$, i.e. $\mathrm{Re}\,(z) < 0$ but $z \neq \infty, 0$. In contrast, since the bonds within the G_r and K_p subgraphs, by themselves, are not directly responsible for the noncompactness of $\mathcal{B}$, it is plausible that homeomorphic expansions of these bonds would not change the nature of $\mathcal{B}$ at $z = 0$.

7. Boundary for L_k limit

Finally, we briefly discuss the boundary $\mathcal{B}$ that results when one takes the limit L_k of equation (2.20), i.e. $k \to \infty$ with r and p fixed, for the families studied in this paper. We consider the nontrivial range $r \geqslant 2$ since for $r = 1$, families typically degenerate into tree graphs with $\mathcal{B} = \emptyset$. For the families studied here for which we have obtained the chromatic polynomials for general k, including $H_{k,r}$, $O_{k,r}$, and $U_{k,r}$, we find that this boundary is simply the unit circle $|q - 1| = 1$. This is easily understood, since one can re-express our formulae for chromatic polynomials in terms of polynomials in $a = q - 1$ using equations (1.6) and (1.7). From equation (1.7), it follows that the chromatic polynomials are of the form of equation (1.2) with a as the quantity entering in terms raised to respective powers proportional to k, together with possible c_0 terms involving $(-1)^k$, and hence, as discussed in our earlier work [12], $\mathcal{B}$ is determined by the condition $|a| = 1$. Hence, $q_c = 2$ and $\mathcal{B}$ has no support for $\mathrm{Re}\,(q) < 0$. Since the locus $|q - 1| = 1$ is compact in the q-plane and since our focus here is on the situation where $\mathcal{B}(q)$ is noncompact in the q-plane, passing through $z = 0$, and the connection with the existence of large-q series for $W_{\rm red}$, the L_k limit is not of primary interest here. We mention, however, that $\mathcal{B}$ divides the q-plane into two regions, $(R_1)_{L_k}$ and $(R_2)_{L_k}$, which are the exterior and interior of the unit circle

$|q-1|=1$ (the subscripts L_k are appended to distinguish these regions from those for the L_r limit). It is straightforward to calculate the W-function in these two regions in the L_k limit of the various families. For example, for the $H_{k,r}$ family (for fixed $r \geqslant 2$),

$$W\left(\left[\lim_{k\to\infty} H_{k,r}\right], q\right) = q-1 \qquad \text{for } q \in (R_1)_{L_k} \tag{7.1}$$

and

$$|W\left(\left[\lim_{k\to\infty} H_{k,r}\right], q\right)| = 1 \qquad \text{for } q \in (R_2)_{L_k}. \tag{7.2}$$

8. Conclusions

In this paper we have presented exact calculations of the zero-temperature partition function, $Z(G,q,T=0)$, and ground-state degeneracy (per site), $W(\{G\},q)$, for the q-state Potts antiferromagnet on a number of families of graphs $\{G\}$ for which the boundary $\mathcal{B}$ of regions of analyticity of W in the complex q-plane is noncompact and has the properties that (i) in the $z=1/q$-plane, the point $z=0$ is a multiple point on $\mathcal{B}$; (ii) $\mathcal{B}$ includes support for $\mathrm{Re}\,(z)<0$; and (iii) $\mathcal{B}$ crosses the imaginary z-axis away from $z=0$. Our results yield insight into the conditions which preclude the existence of large-q Taylor series expansions for the reduced function $W_{\mathrm{red}} = q^{-1}W$. This insight is valuable since large-q expansions, where they exist, are of great utility in obtaining approximate values of the exponent of the ground state entropy, W.

Acknowledgment

This research was supported in part by the NSF grant PHY-93-09888.

References

[1] Potts R B 1952 *Proc. Camb. Phil. Soc.* **48** 106
[2] Wu F Y 1982 *Rev. Mod. Phys.* **54** 235
Wu F Y 1983 *Rev. Mod. Phys.* **55** 315 (erratum)
[3] Birkhoff G D 1912 *Ann. Math.* **14** 42
[4] Read R C 1968 *J. Comb. Theor.* **4** 52
Read R C and Tutte W T 1988 Chromatic polynomials *Selected Topics in Graph Theory 3* ed L W Beineke and R J Wilson (New York: Academic)
[5] Tutte W T 1984 Graph theory *Encyclopedia of Mathematics and its Applications* vol 21, ed G C Rota (New York: Addison-Wesley)
[6] Harary F 1969 *Graph Theory* (Reading, MA: Addison-Wesley)
Biggs N L 1993 *Algebraic Graph Theory* (Cambridge: Cambridge University Press)
[7] Pauling L 1960 *The Nature of the Chemical Bond* (Ithaca, NY: Cornell University Press) p 466
[8] Lieb E H and Wu F Y 1972 *Phase Transitions and Critical Phenomena* vol 1, ed C Domb and M S Green (New York: Academic) p 331
[9] Some related early work is in Beraha S, Kahane J and Weiss N 1980 *J. Comb. Theory* B **28** 52
Baxter R J 1987 *J. Phys. A: Math. Gen.* **20** 5241
Read R C and Royle G F 1991 *Graph Theory, Combinatorics, and Applications* vol 2 (New York: Wiley) p 1009
[10] Read R C and Royle G F 1991 *Graph Theory, Combinatorics, and Applications* vol 2 (New York: Wiley) p 1009
[11] Shrock R and Tsai S-H 1997 *J. Phys. A: Math. Gen.* **30** 495
[12] Shrock R and Tsai S-H 1997 *Phys. Rev.* E **55** 5165
Shrock R and Tsai S-H 1997 *Phys. Rev.* E **56** 1342
[13] Shrock R and Tsai S-H 1997 *Phys. Rev.* E **56** 3935

[14] Shrock R and Tsai S-H 1997 *Phys. Rev.* E **55** 6791
Shrock R and Tsai S-H 1997 *Phys. Rev.* E **56** 2733
Tsai S-H 1998 *Phys. Rev.* E **57** 2686
[15] Shrock R and Tsai S-H 1997 *Phys. Rev.* E **56** 4111
[16] Roček M, Shrock R and Tsai S-H 1998 *Physica* A **252** 505
Roček M, Shrock R and Tsai S-H 1998 *Physica* A **259** 367
Shrock R and Tsai S-H 1998 *Physica* A **259** 315
Shrock R and Tsai S-H 1998 *Phys. Rev.* E **58** 4332
[17] Nagle J F 1971 *J. Comb. Theor.* B **10** 42
Nagle J F 1968 *J. Math. Phys.* **9** 1007
[18] Baker G A Jr 1971 *J. Comb. Theor.* B **10** 217
[19] Kim D and Enting I G 1979 *J. Comb. Theor.* B **26** 327
[20] Lefschetz S 1953 *Algebraic Geometry* (Princeton, NJ: Princeton University Press)
Hartshorne R 1977 *Algebraic Geometry* (New York: Springer)
[21] Tsai S-H 1998 *PhD Thesis* State University of New York
[22] Read R C and Whitehead E G *Discrete Math.* at press. We thank Professor Read for kindly giving us a copy of this preprint
[23] Martin P P 1991 *Potts Models and Related Problems in Statistical Mechanics* (Singapore: World Scientific)
[24] Chen C N, Hu C K and Wu F Y 1996 *Phys. Rev. Lett.* **76** 169
Wu F Y *et al* 1996 *Phys. Rev. Lett.* **76** 173
[25] Matveev V and Shrock R 1996 *Phys. Rev.* E **54** 6174
[26] Schrock R and Tsai S-H 1998 *Preprint* ITP-SB-98-17